BJP British Journal of Pharmacology

DOI:10.1111/bph.13173
www.brjpharmacol.org

RESEARCH PAPER

Effect of polyphenolic phytochemicals on ectopic oxidative phosphorylation in rod outer segments of bovine retina

Daniela Calzia[1], Michele Oneto[1], Federico Caicci[2], Paolo Bianchini[3], Silvia Ravera[1], Martina Bartolucci[1], Alberto Diaspro[3], Paolo Degan[4], Lucia Manni[2], Carlo Enrico Traverso[5] and Isabella Panfoli[1]

[1]*Department of Pharmacy-DIFAR, Biochemistry and Physiology Laboratory, University of Genoa, Genova, Italy,* [2]*Department of Biology, Università di Padova, Padova, Italy,* [3]*Department of Nanophysics, Istituto Italiano di Tecnologia, Genova, Italy,* [4]*UOC Mutagenesi, IRCCS Azienda Ospedaliera Universitaria San Martino – Istituto Nazionale per la Ricerca sul Cancro, Genova, Italy, and* [5]*Clinica Oculistica, Di.N.O.G.M.I., University of Genoa, IRCCS Azienda Ospedaliera Universitaria San Martino – Istituto Nazionale per la Ricerca sul Cancro, Genova, Italy*

Correspondence
Dr Daniela Calzia, Department of Pharmacy-DIFAR, Biochemistry and Physiology Laboratory, University of Genoa, V.le Benedetto XV,3, Genova 16132, Italy. E-mail: dcalzia@gmail.com

Received
7 October 2014
Revised
24 March 2015
Accepted
20 April 2015

BACKGROUND AND PURPOSE

The rod outer segments (OS) of the retina are specialized organelles where phototransduction takes place. The mitochondrial electron transport complexes I–IV, cytochrome *c* and F_oF_1-ATP synthase are functionally expressed in the OS disks. Here, we have studied the effect of some polyphenolic compounds acting as inhibitors of mitochondrial ATPase/synthase activity on the OS ectopic F_oF_1- ATP synthase. The mechanism of apoptosis in the OS was also investigated studying the expression of cytochrome *c*, caspase 9 and 3 and Apaf-1.

EXPERIMENTAL APPROACH

We prepared OS from fresh bovine retinae. Semi-quantitative Western blotting, confocal and electron microscopy, and cytofluorimetry were used along with biochemical analyses such as oximetry, ATP synthesis and hydrolysis.

KEY RESULTS

Resveratrol and curcumin plus piperine inhibited ATP synthesis and oxygen consumption in the OS. Epigallocatechin gallate and quercetin inhibited ATP hydrolysis and oxygen consumption in the OS. Malondialdehyde and hydrogen peroxide were produced in respiring OS in the presence of substrates. Cytochrome *c* was located inside the disk membranes. Procaspase 9 and 3, as well as Apaf-1 were expressed in the OS.

CONCLUSIONS AND IMPLICATIONS

These polyphenolic phytochemicals modulated the F_oF_1-ATP synthase activity of the the OS reducing production of reactive oxygen intermediates by the OS ectopic electron transport chain. Polyphenols decrease membrane peroxidation and cytochrome *c* release from disks, preventing the induction of caspase-dependent apoptosis in the OS Such effects are relevant in the design of protection against functional impairment of the OS following oxidative stress from exposure to intense illumination.

Abbreviations

AMD, age-related macular degeneration; Ap5A, di(adenosine)-5-penta-phosphate; ATP synthase, F_oF_1-ATP synthase; CLSM, confocal laser scanning microscopy; Cyt *c*, cytochrome *c*; DR, diabetic retinopathy; EGCG, epigallocatechin gallate; ETC, electron transport chain; OS, outer segment; PUFA, polyunsaturated fatty acids; ROI, reactive oxygen intermediates; RP, retinitis pigmentosa; TEM, transmission electron microscopy

Tables of Links

TARGETS
Enzymes
F_oF_1-ATP synthase
Caspase 3
Caspase 9

LIGANDS
EGCG, epigallocatechin gallate
Resveratrol (RVX 208)
Ap5A, di(adenosine)-5-penta-phosphate
Piperine
Curcumin

These Tables list key protein targets and ligands in this article which are hyperlinked to corresponding entries in http://www.guidetopharmacology.org, the common portal for data from the IUPHAR/BPS Guide to PHARMACOLOGY (Pawson *et al.*, 2014) and are permanently archived in the Concise Guide to PHARMACOLOGY 2013/14 (Alexander *et al.*, 2013).

Introduction

Oxidative stress is a major factor in the pathogenesis of retinal degenerative diseases, including photoreceptor-related pathologies such as age-related macular degeneration (AMD) (Janik-Papis *et al.*, 2009) and diabetic retinopathy (DR) (Baynes, 1991; Gupta *et al.*, 2011). Because the retina is characterized by higher metabolic rates, compared with other tissues, with photoreceptors consuming about four times more oxygen than the other retinal or CNS cells (Linsenmeier *et al.*, 1998), oxygen is pivotal for the photoreceptor survival (Wangsa-Wirawan and Linsenmeier, 2003). There is a high level of oxygen utilization in the dark-adapted outer retina (Wangsa-Wirawan and Linsenmeier, 2003). This is consistent with our previous proteomic and biochemical analyses reporting the expression and activity of an ectopic F_oF_1-ATP synthase (ATP synthase) as well as of the electron transport chain (ETC) and cytochrome *c* (Cyt *c*) in isolated rod outer segment (OS) disks (Panfoli *et al.*, 2008; 2009). The OS themselves are possibly responsible for the high oxygen consumption of the outer retina (Stefansson, 2006). Recent data, showing that oxidative stress induced by exposure to short wavelength light (blue light) exerts its effects more on the OS than on the inner segment (IS) of the photoreceptors (Roehlecke *et al.*, 2013), have reinforced this idea. Not only the IS, which contains mitochondria, but also the OS, is a source of reactive oxygen intermediates (ROI) that mediate blue light-induced cytotoxicity (Roehlecke *et al.*, 2013). The ETC is a major source of ROI (Genova *et al.*, 2008) and the lipids of the rod OS membranes are susceptible to oxidation as they have a very high content of polyunsaturated fatty acids (PUFA). When oxidized, PUFA initiate cytotoxic redox chain reactions leading to ROI production and oxidative stress (Fliesler and Anderson, 1983).

It is known that disks die from apoptosis, for which a causative explanation is still lacking (Fain *et al.*, 2001). One pathway triggering caspase-mediated apoptosis is the formation of apoptosomes, involving caspase 9 activation by Cyt *c* and their binding to cytosolic Apaf-1 (Blanch *et al.*, 2014). Our previous proteomic analysis showed that Cyt *c* was expressed in the disks and that ATP synthase in the disk was outward facing (Panfoli *et al.*, 2008). Considering that the sidedness of Cyt *c* is opposite to that of the F_1 moiety of ATP synthase, this raises the possibility that exposure of the disk membrane to oxidative stress due to any over-functioning of the ETC may allow Cyt *c* to escape from the intradiscal space.

Some polyphenolic phytochemicals are natural compounds displaying a potent antioxidant action. They also act as ATP synthase inhibitors (Zheng and Ramirez, 2000). Mitochondrial ATP synthase displays two functional domains. F_1, a water-soluble catalytic complex consisting of five subunits (α_3, β_3, γ, δ and ε), with the catalytic site located on the β subunit, and F_o, consisting of several membrane proteins (a, b, c, d, e, F6 and A6L) thereby comprising the oligomycin sensitivity-conferring protein (Pedersen and Amzel, 1993; Boyer, 1997). As protons flow down their concentration gradient, the c-subunit ring of F_o rotates clockwise driving ATP synthesis (Stock *et al.*, 1999). Upon counter-clockwise movement it performs ATP hydrolysis (ATPase activity). Because of its complex structure, ATP synthase is inhibited by a number of different natural and synthetic inhibitors. The natural inhibitor is the protein inhibitor of F_1 (IF_1), a basic protein binding F_1 under de-energized conditions, designed to preserve the cellular ATP (Zanotti *et al.*, 2009). Exogenous inhibitors of ATP synthase have been described, including efrapeptin, oligomycin, aurovertin B (Huang *et al.*, 2008) and azide (Linnett and Beechey, 1979). The binding pocket for the F_1-targeting inhibitor efrapeptin is localized in α, β and γ subunits, while that for aurovertin B is mainly in the β subunit (van Raaij *et al.*, 1996).

Resveratrol is a natural stilbene phytoalexin inhibitor of ATP synthase that targets the F1 component. It affects both ATPase and ATP synthase activity by binding between α and β subunits (Gledhill *et al.*, 2007). A class of flavonoid-related

polyphenolic compounds produced in plants, the flavones, including quercetin, kaempferol, morin and apigenin, also inhibit the ATP hydrolytic, but not the ATP synthetic, activity of mitochondrial ATP synthase (Lang and Racker, 1974). Kaempferol, morin and apigenin display an inhibitory action on the ATPase activity similar to that of quercetin, even though the latter shows about half the inhibitory potency (Zheng and Ramirez, 2000). The catechins are a separate class of polyphenolic compounds abundant in green tea (Higdon and Frei, 2003) and include epicatechin, epigallocatechin and epigallocatechin gallate (EGCG). The latter two are inhibitors of the ATP hydrolysis (Zheng and Ramirez, 2000). EGCG has extremely strong antioxidative properties (Lee *et al.*, 2003). Curcumin, the active ingredient of the Indian curry spice, is a polyphenol extracted from turmeric (*Curcuma longa*), a spice widely used in South Asian foods. It also acts as an inhibitor of the F_1 catalytic headpiece (Zheng and Ramirez, 2000).

Here, we report that resveratrol, curcumin, quercetin and EGCG inhibit the ectopic ATP synthase expressed in the OS, affecting either its ATPase or ATP synthase activity or both. They also inhibit the oxygen consumption of the OS. This appears consistent with the hypothesis that the OS express a functional ATP synthase and also with the beneficial effect these compounds exert on many retinal pathologies (Panfoli *et al.*, 2012). We also found Cyt *c* inside the disk and of procaspase 9 and 3, and Apaf-1 in the OS.

Methods

Sample preparations

Extraction of retinas. Retinas were extracted as previously described (Bianchini *et al.*, 2008). Briefly, the eye semicup, including the retina, from freshly enucleated bovine eyes (obtained from a local certified slaughterhouse) after vitreous and lens removal, were incubated for 10 min with mammalian Ringer solution [composition: 0.157 M NaCl, 5 mM KCl, 7 mM Na_2HPO_4, 8 mM NaH_2PO_4, 0.5 mM $MgCl_2$, 2 mM $CaCl_2$, pH 6.9, plus protease inhibitor cocktail (Sigma-Aldrich, St. Louis, MO, USA) and 50 $\mu g \cdot mL^{-1}$ ampicillin]. Each retina was then cut free of the optic nerve with scissors and collected.

Purified bovine rod OS preparations. Purified bovine rod OS were prepared under dim red light at 4°C from 14 retinas, by sucrose/Ficoll continuous gradient centrifugation (Schnetkamp, 1981; Panfoli *et al.*, 2008) in the presence of protease inhibitor cocktail (Sigma-Aldrich) and ampicillin (100 $\mu g \cdot mL^{-1}$). OS preparations were characterized for integrity of plasma membrane as reported earlier (Schnetkamp, 1981). OS homogenates were obtained by Potter-Elvehjem homogenization on ice in 1:1 (w/v) hypotonic medium (5 mM Tris-HCl, pH 7.4 plus protease inhibitor cocktail and 100 $\mu g \cdot mL^{-1}$ ampicillin).

Osmotically intact OS disk preparations. Osmotically intact disks were prepared by Ficoll flotation (Schnetkamp and Daemen, 1982) from purified OS. After letting the OS burst for 3 h in 5% Ficoll solution in distilled water with 70 $\mu g \cdot mL^{-1}$ leupeptin and 100 $\mu g \cdot mL^{-1}$ ampicillin at 4°C in distilled water sample was layered onto Ficoll and the suspension centrifuged for 2 h at 40 000–100 000× *g*. in a Beckman FW-27 rotor (Beckman Coulter, Brea, CA, USA). Disks were collected at the interface between water and Ficoll under sterile conditions.

Both OS and disk purification procedures were carried out in the absence of cyclosporin A and 2-aminoethoxydiphenyl borate, inhibitors of the opening of the mitochondrial permeability transition pore (MPTP) Berman *et al.*, 2000; Chinopoulos *et al.*, 2003). Such conditions promote the formation of MPTPs in contaminant mitochondria, if any, so that these would not be functional.

Isolation of retinal mitochondria-enriched preparations. Bovine retinal mitochondria-enriched fractions were isolated by differential centrifugation technique from residual retinae, after OS preparation as previously reported (Panfoli *et al.*, 2009). The pellet was stored at –80°C. All steps were performed at 4°C.

Transmission electron microscopy (TEM)

For immunostaining of sections, the post-embedding immunogold method was applied. Sections were first treated with blocking solution (1% BSA, 0.1% Tween 20, PBS 1×), then incubated with mouse monoclonal anti-rhodopsin (Rh; diluted 1:100; Sigma-Aldrich) or goat polyclonal anti-caspase-3 p11 (diluted 1:400; Santa Cruz Biotechnology, Inc., Dallas, TX, USA) or rabbit polyclonal or goat polyclonal anti-caspase-9 p10 (diluted 1:100; Santa Cruz Biotechnology, Inc.) anti-ATP synthase β-subunit (diluted 1:50; Sigma-Aldrich) overnight at 4°C. Ab binding was detected using a secondary Ab rabbit anti-goat IgG (British BioCell International, BBI Solutions, Cardiff, UK; diluted 1:100) coupled to gold particles (10 nm) or goat anti-mouse IgG (British BioCell International; diluted 1:100) coupled to gold particles (40 nm) or goat anti-rabbit IgG (Sigma-Aldrich; diluted 1:100) coupled to gold particles (10 nm). Sections were analysed at a FEI Tecnai G12 transmission electron microscope (FEI, Hillsboro, OR, USA) operating at 100 KV. In negative controls, the pre-immune serum was applied to the sections instead of the specific primary Ab. The images were taken with Tietz TVIPS F114 (Tietz Video & Image Processing Systems GmbH, Gauting, Germany) and OSIS Veleta cameras (Olympus Soft Imaging Solutions, Cincinnati, OH, USA), collected and typeset in Corel Draw X3 (Corel Corporation, Ottawa, ON, Canada). Controls were performed by omitting primary Ab, which resulted in the absence of cross-reactivity (data not shown).

Electrophoresis, semi-quantitive Western blot (WB) and quantification

Denaturing electrophoresis (SDS-PAGE) was performed using a Laemmli (Laemmli, 1970) protocol on gradient 8–20% gels. After SDS-PAGE, samples were electrophoretically transferred onto nitrocellulose membranes and incubated with primary antibodies (Santa Cruz Biotechnology, Inc.): mouse monoclonal anti-bovine rhodopsin (sc-57432) (Santa Cruz Biotechnology, Inc.), rabbit polyclonal antibody against Cyt *c* (sc-13561) (Santa Cruz Biotechnology, Inc.), rabbit polyclonal antibody against procaspase 9 (sc-7885) (Santa Cruz Biotechnology, Inc.), goat polyclonal anti-procaspase 3 antibody (sc-1224) and rabbit polyclonal antibody against Apaf-1 A 8469 (Sigma-Aldrich). Anti-rhodopsin was diluted in 1:1000 PBS, anti-

procaspase 9, anti-procaspase 3 and anti-Cyt *c* were diluted in 1:200 PBS while anti-Apaf-1 was diluted in 1:500 PBS. Secondary HRP-conjugated anti-mouse IgG, anti-rabbit and anti-goat IgG antibodies (Sigma-Aldrich) were diluted in 1:10 000 PBS. Quantitative densitometry was performed with Chemi-Doc XRS + (Bio-Rad Laboratories, Hercules, CA, USA).

Confocal laser scanning microscopy (CLSM) of disks

Disks (60 μg protein per 50 μL) were marked in batches as reported (Ravera *et al.*, 2007). A total of 2 $\mu g \cdot mL^{-1}$ of anti-Cyt *c* were used as primary antibodies. Secondary antibodies were Alexa 488-labelled anti-rabbit IgG (Molecular Probes, Life Technologies, Carlsbad, CA, USA). CLSM imaging was performed as reported (Panfoli *et al.*, 2009) on an inverted LEICA TCS SP5 AOBS confocal laser scanning microscope (Leica Microsystems CMS, Mannheim, Germany). Control samples, incubated with secondary antibodies only, showed a negligible immunoreactivity (data not shown).

ATP synthesis assay in rod OS

The formation of ATP from ADP and inorganic phosphate was performed in rod OS according to Mangiullo *et al.* (2008). OS (0.04 mg protein·mL^{-1}) were incubated for 5 min at 37°C in 50 mM Tris/HCl (pH 7.4), 5 mM KCl, 1 mM EGTA, 5 mM $MgCl_2$, 0.6 mM ouabain, 0.25 mM di(adenosine)-5-pentaphosphate (Ap5A, adenylate kinase inhibitor) and 25 $\mu g \cdot mL^{-1}$ ampicillin. ATP synthesis was induced by adding 5 mM KH_2PO_4, 20 mM succinate, 0.35 mM NADH and 0.1 mM ADP at the same pH of the mixture. After stopping the reaction with 7% perchloric acid final concentration, the ATP concentration in each sample was measured in a luminometer (Lumi-Scint, Bioscan Inc, Washington, DC, USA) by the luciferin/luciferase chemiluminescent method with ATP standard solutions between 10^{-9} and 10^{-7} M for calibration (Roche Diagnostics Corporation, Indianapolis, IN, USA). Neutralized and clarified supernatant was added to a mixture containing 2 mM $MgCl_2$, 0.5 mM NADP, 5 mM glucose, 100 mM Tris/HCl, pH 7.4 and 7 $U \cdot mL^{-1}$ of a mix of hexokinase and glucose-6-phosphate dehydrogenase (Roche Diagnostics Corporation). $NADP^+$ reduction was followed in a dual-beam spectrophotometer (UNICAM UV2, Analytical S.n.c., Borgotaro (PR), Italy). Where necessary, the incubation medium contained 30 μM resveratrol or curcumin plus piperine at different concentrations (200, 100, 50 and 25 μM).

Hydrogen peroxide production assay

Production of hydrogen peroxide (H_2O_2) was evaluated using luminometric analysis. Samples of OS homogenate (70 μg) was incubated for 10 min at 37°C in 50 mM Tris/HCl (pH 7.4), 5 mM KCl, 1 mM EGTA, 5 mM $MgCl_2$, 0.6 mM ouabain, with 0.3 mM NADH or 20 mM succinate or 10 mM pyruvate 5 mM malate (pyr/malate). After incubation, samples were centrifuged and after the addition of peroxidase and luminol, H_2O_2 production was evaluated in the supernatant by luminometry. Concentration of H_2O_2 was measured using a calibration curve with H_2O_2 standard solutions between 10 and 40 μM.

Malondialdehyde (MDA) measurements

MDA concentration was evaluated in OS homogenates (70 μg) using the thiobarbituric acid reactive substances (TBARS) assay kit (OxiSelect™ TBARS Assay Kit, Cell Biolabs, Inc., San Diego, CA, USA), a tool for the direct quantitative measurement of MDA in biological samples. Samples or MDA standards were first reacted with TBA at 95°C and then assayed spectrophotometrically at 532 nm. The MDA content in samples was determined by comparison with a MDA standard curve.

ATP hydrolysis assay in rod OS

The ATPase activity of rod OS was assayed by the pyruvate kinase, lactate dehydrogenase system in which hydrolysis of ATP is coupled to the oxidation of NADH followed at 340 nm (ε_{340} for NADH = 6.22 $mM^{-1} \cdot cm^{-1}$; Bucher and Pfleiderer, 1955). Rod OS (40 μg protein·mL^{-1}) were added to a reaction mixture [50 mM HEPES, pH 7.4, 100 mM KCl, 150 mM NaCl, 1 mM EGTA, 2.5 mM $MgCl_2$, 0.8 mM ouabain, 0.15 mM NADH, 0.4 mM Ap5A (adenylate kinase inhibitor), 1.5 mM phosphoenolpyruvate, pyruvate kinase and lactate dehydrogenase and 25 $\mu g \cdot mL^{-1}$ ampicillin]. ATP hydrolysis was then induced by adding 1 mM ATP. Absorbance values were measured every minute for 10 min. Where necessary, EGCG or quercetin at different concentrations (2, 10, 25, 50, 75 and 100 μM) was added to the reaction mixture.

Oxygraphic measurements

Oxygen consumption by rod OS (40 μg protein per 1.7 mL) was measured at 23°C in a closed chamber using a thermostatically controlled oxygraph apparatus equipped with an amperometric electrode (Unisense–Microrespiration, Unisense A/S, Aarhus, Denmark) under continuous electromagnetic stirring conditions (Panfoli *et al.*, 2009). A specific software (MicOx, Unisense A/S) was used to convert data in Excel files. OS were previously diluted in 3:1 ultrapure water, then added to the mixture by means of an Hamilton syringe, which caused a partial disruption of OS, allowing substrates to permeate. Incubation medium was 50 mM HEPES, pH 7.3, 100 mM KCl, 2 mM $MgCl_2$, 5 mM KH_2PO_4, 25 $\mu g \cdot mL^{-1}$ ampicillin and 0.3 mM Ap5A to inhibit adenylate kinase (Aicardi and Solaini, 1982). Respiring substrates were 0.3 mM NADH and 20 mM succinate. When necessary, curcumin (100 μM), plus piperine (100 μM), EGCG (100 μM) or quercetin (100 μM) were added.

Cytofluorimetric measurements

Cytofluorimetric measurements of OS membrane polarization were performed using 5,5′,6,6′-tetrachloro-1,1′,3,3′-tetraethylbenzimidazolcarbocyanineiodide (JC-1) and tetramethylrhodamine methyl ester (TMRM; Molecular Probes, Life Technologies). Changes in mitochondrial membrane potential can be evaluated using the lipophilic cationic probes JC-1 and TMRM, which reversibly change their colour from green to orange as this potential increases. This is due to the reversible formation of JC-1 aggregates upon membrane polarization that causes shifts in emission of JC-1 monomeric from 530 to 590 nm corresponding to the emission of J aggregates when excited at 490 nm. The green and orange/red emissions are detected in separate channels in the flow cytometer. For TMRM, the green fluorescence signal was collected through a 530/30 band pass filter and the orange fluorescence was collected through a 585/42 band pass filter. OS were washed in PBS and resuspended in 50 mL HEPES

buffer (10 mM HEPES, 135 mM NaCl, 5 mM $CaCl_2$) and stained for 20 min with JC-1 (2.5 mg·mL^{-1}) or TMRM (final concentration 200 nM) and kept at room temperature, washed with PBS and resuspended in a total volume of 400 µL of PBS. Flow cytometry was performed in a CyAn ADP cytometer (Beckman Coulter) equipped with three laser lamps. The plot of all physical parameters (forward scatter vs. side scatter) is used to set the gate that limits debris and aggregates. Ten thousand cells per sample are routinely analysed and the results are reported as the percentage of cells relative to the relevant control that display a fluorescence shift. In a typical experiment, each sample is prepared either stained or unstained for both drug-free (untreated samples) and drug-treated samples.

Data analysis

Results are expressed as mean ± SD and *n* refers to the number of assays in any particular condition. In ATP synthesis/hydrolysis assays, statistical analysis was performed using Student's *t*-test to compare data obtained using different concentrations of polyphenols to those obtained in control samples. Results were considered significant if $P < 0.05$.

Materials

Ampicillin, Ap5A, curcumin, EGCG, oligomycin, ouabain, piperine, quercitin, and resveratrol were all supplied by Sigma-Aldrich (St. Louis, MO, USA).

Results

As we had found active ATP synthase in isolated purified rod OS disks (Panfoli *et al*., 2008; 2009; Calzia *et al*., 2013a) and others had reported that polyphenolic phytochemicals act as inhibitors of mitochondrial ATP synthase and ATPase activity (Zheng and Ramirez, 2000), we were prompted to test the effects of some of these compounds both on the ATP production or hydrolysis in the OS. The bovine retinal rod OS were purified (Schnetkamp and Daemen 1982) in the form of intact OS detached from IS, still containing the cytosol, plasma membrane and disk saccules, as *in vivo*. Our previous characterization of the OS fraction excluded contamination by mitochondria and IS (Calzia *et al*., 2013a) and recent data demonstrate that the purified OS consume oxygen and synthesize ATP through extra-mitochondrial oxidative phosphorylation (Calzia *et al*., 2013a).

Here, we performed immunogold TEM imaging of the bovine retina. A colocalization of rhodopsin with the ATP synthase β-subunit was found in OS (Figure 1A). Figure 1B is a magnification of a portion of double-labelled rod OS showing colocalization of the rhodopsin signal (40 nm diameter gold particles) with the ATP synthase signal (10 nm diameter gold particles). Figure 1C shows a mitochondrion of the IS of the same double-labelled retina, enlarged in Figure 1D, displaying the presence of only the ATP synthase signal.

Data from Western blot analysis in Figure 2 confirmed the results shown in Figure 1, that rhodopsin was present in the OS (Figure 2A), but not in the mitochondria used as negative control. The ATP synthase β-subunit was present in both OS and mitochondria (Figure 2B) as confirmed by densitometric analysis (Figure 2C).

The ATP synthase was catalytically active in the OS and Figure 3 shows ATP synthesis by OS homogenates. A maximal activity of 0.430 ± 0.060 µmol ATP produced per min·mg^{-1} of protein was detected in the presence of 0.35 mM NADH, 10 mM succinate and 0.3 mM ADP. ATP synthesis was specific because it was inhibited by oligomycin (90%), a classical mitochondrial ATP synthase inhibitor. This ATP synthesis was also inhibited by resveratrol (98%, Figure 3).

In order to test the ability of resveratrol to impair the disk membrane proton potential (Bianchini *et al*., 2008), this compound was also used in cytofluorimetric analyses of OS previously labelled with TMRM or JC-1, two mitochondrial membrane potential probes. Table 1 reports the results

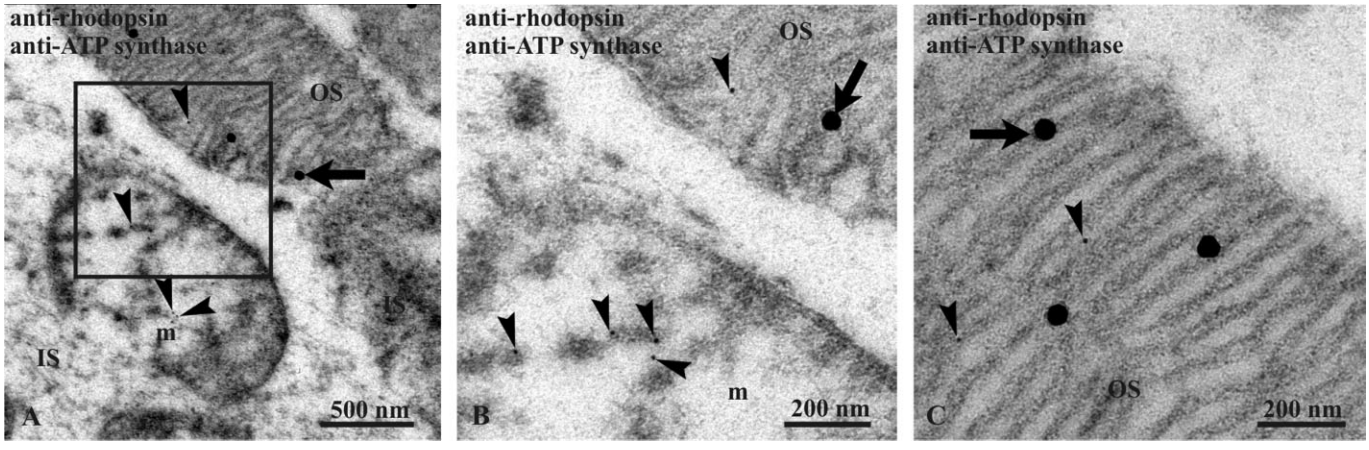

Figure 1

TEM of bovine retina, searching for ATP synthase expression. (A–B) Bovine retina double-labelled with antibodies against rhodopsin (Rh; large, 40 nm width gold particles; arrows) and against the β subunit of ATP synthase (small, 10 nm width gold particles; arrowheads). Squared area in (A) is enlarged in (B) to show the detail of OS, characterized by colocalization of the signals for Rh and for ATP and a mitochondria (m) in an adjacent IS, where only ATP synthase is expressed. (C) Detail of an OS.

obtained using OS homogenates in the presence of NADH and succinate or after the addition of resveratrol (30 μM). Controls display a uniform signal for both TMRM and JC-1, indicating the presence of a membrane electrochemical potential, as reported earlier (Panfoli *et al.*, 2009). Incubation for 30 min with resveratrol did not decrease membrane potential. Measurements carried out at different time points up to 1 h did not show a significant decrease in membrane polarization (data not shown).

The effect of curcumin alone or associated with piperine on OS ATP production is shown in Figure 4A. Curcumin (100μM) inhibited ATP synthesis when used alone but combination with piperine a polyphenol from black pepper (also at 100 μM) increased inhibition. The effects of this combination (using equal concentrations) were concentration-dependent (Figure 4B).

Having previously reported that ATP synthase and ATPase in the OS represent the same protein, that is the ectopic ATP synthase (Calzia *et al.*, 2013b), ATPase activity was assayed in the presence of EGCG and quercetin to test their inhibitory action on OS ATP hydrolytic activity, as reported for mitochondrial ATP synthase (Zheng and Ramirez, 2000). As shown in Figure 5A and 5B, either compound exhibited concentration-dependent inhibition of ATP hydrolysis. Although the OS in our experiments were checked for purity and appeared to be devoid of IS and plasma membrane proteins, the ATPase assay was performed in the presence of ouabain, an inhibitor of Na^+/K^+ATPase, and EDTA, an inhibitor of Ca^{2+}-ATPase in order to prevent any contribution from other ATPase activities.

Polyphenolic compounds also affected the rates of oxygen consumption by the OS. Representative tracings of amperometric recordings of coupled respiratory rates are shown in

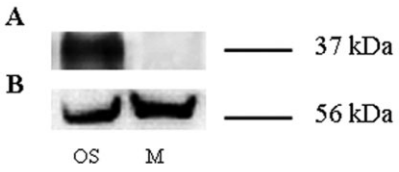

C

	Relative optical density	
	OS	Mitochondria
Rhodopsin	7.5±1.3	0
B subunit F_0F_1-ATP synthase	10.5±1.54	9.41±1.37

Figure 2

Characterization of isolated rod OS by semi-quantitative Western blot analysis. (A and B) Semi-quantitative Western blot with antibodies against rhodopsin (Rh) and the β subunit of ATP synthase. The samples are from isolated OS and mitochondria-enriched fraction (M). (C) Densitometric analysis made with ChemiDoc software (Bio-Rad Laboratories). Each panel is representative of at least five experiments

Table 1

Membrane potential measurements of OS membranes by cytofluorimetric analysis

	OS control	OS + RV
TMRM	97.3 ± 4.5	96.1 ± 5.3
JC-1	91.4 ± 5.9	89.8 ± 6.3

Data shown are from polarized OS, as controls, compared with OS treated with resveratrol (RV; 30μM). Purified OS (2.5 mg·mL^{-1}) was incubated with 0.29 mM NADH and 20 mM succinate. They were stained with either TMRM or JC-1 (OS control). Values shown are % of cells stained positively (mean ± S.D; n = 4). Incubation with resveratrol ()S+RV) did not significantly change the proportion of stained cells, showing no change in membrane potential of OS preparations.

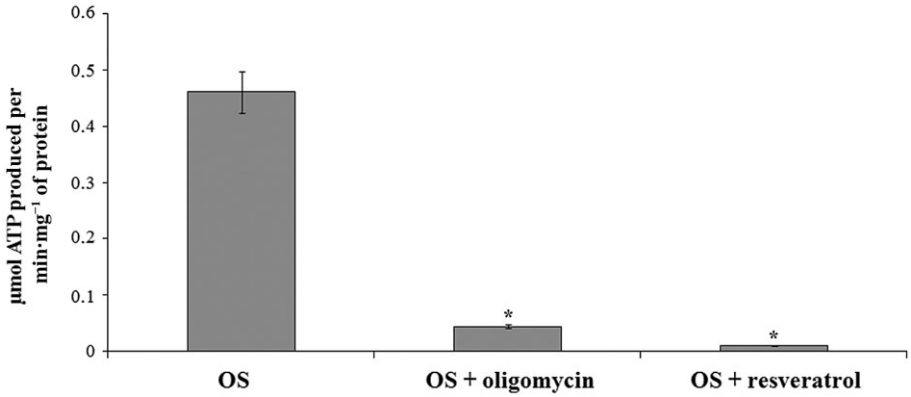

Figure 3

ATP synthesis in purified OS with oligomycin and resveratrol. Histogram shows ATP formation over 1 min at 37°C, pH 7.3, by OS (40 μg·mL^{-1}). Addition of 10 μM oligomycin and 30 μM resveratrol inhibited ATP production by 90% and 98% respectively. Data shown are means ± SD n = 4. *P < 0.01, paired Student's t-test.

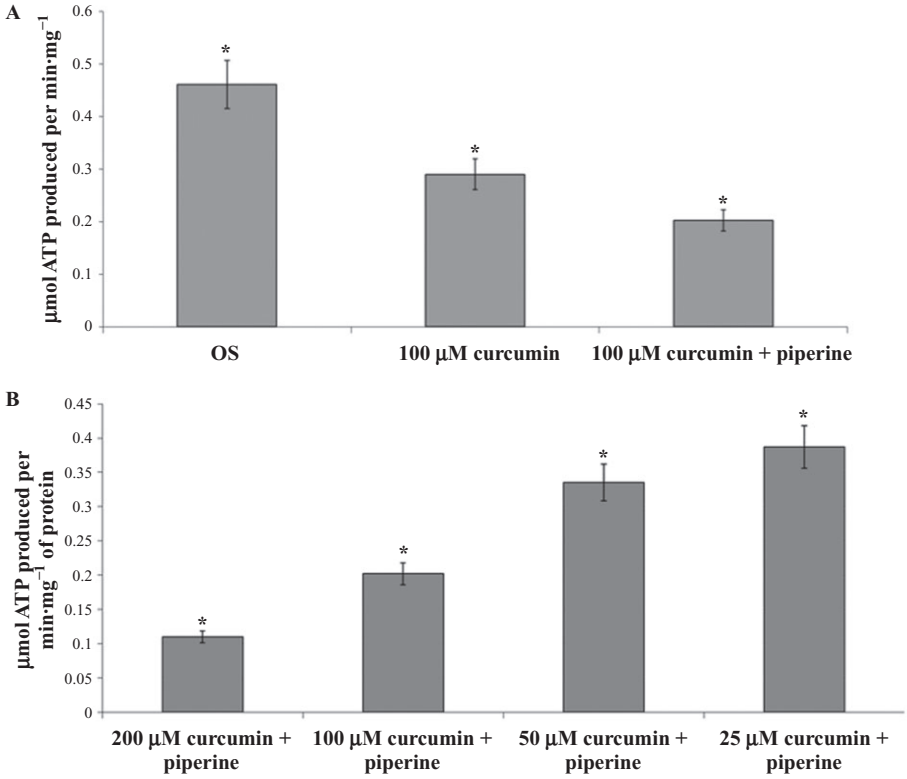

Figure 4

ATP synthesis in purified OS with curcumin and piperine. Histogram shows ATP formation over 1 min at 37°C, pH 7.3, by OS (40µg·mL^{-1}). (A) Addition of 100 µM curcumin and 100 µM curcumin plus 100 µM piperine inhibited ATP production. (B) Addition of combinations of 200, 100, 50 or 25 µM curcumin and piperine inhibit ATP synthesis. Data shown are means ± SD $n = 4$. *$P < 0.01$, paired Student's *t*-test.

Table 2

Hydrogen peroxide production by preparations of rod OS

	nmol H_2O_2·min^{-1}·mg^{-1}
OS + pyr/mal	5.6
OS + NADH	10.7
OS + succinate	8.3

The results in this Table show that the OS preparations were able to generate hydrogen peroxide from a range of different respiration substrates, such as pyruvate/malate mixture (pyr/mal), NADH and succinate. Data shown are means +SD; $n = 5$

Figure 6, as measured in the OS (40 µg per 1.7 mL) in the presence of NADH and succinate as respiratory substrates. Addition of 200 µM curcumin plus 200 µM piperine (Figure 6A) or 100 µM EGCG (Figure 6B) or 100 µM quercetin (Figure 6C) depressed ADP-stimulated oxygen consumption decreased by about 61, 76 and 78% respectively. We have already reported that resveratrol inhibits the OS oxygen consumption (Calzia *et al.*, 2013a).

The ability of OS to produce H_2O_2 was measured in the presence of different respiring substrates (pyruvate/malate, NADH, succinate). Data are reported in Table 2.

Because disk lipids might be peroxidized as a consequence of the ROI production by the ectopic ETC, MDA production in the OS membranes was also evaluated. In the presence of NADH, MDA production was 0.14 nmol MDA·min^{-1}·mg^{-1}, while in the control samples, without NADH, it was 0.05 nmol MDA·min^{-1}·mg^{-1}.

We have earlier proteomic data for the expression of Cyt *c* in isolated purified disks (Panfoli *et al.*, 2008) and here we confirmed its presence inside the isolated OS disks. CLSM imaging of disks labelled with anti-Cyt *c* antibody, performed according to our labelling technique (Ravera *et al.*, 2007), showed no labelling of disks. In fact no fluorescent signal was detectable (Figure 7A), although the disks were visible in the transmission image (Figure 7B). By contrast, Western blots showed that Cyt *c* was expressed in the disks as well as in mitochondria used as positive control (Figure 7D) and that Cyt *c* sidedness is typically opposite to that of the F_1 moiety of ATP synthase. Disks stained positively for the presence of rhodopsin (Figure 7C). The results were summarised by densitometric analysis (Figure 7E).

Expression of Cyt *c* inside the disk implies that any damage to the disk membrane, such as PUFA oxidation by

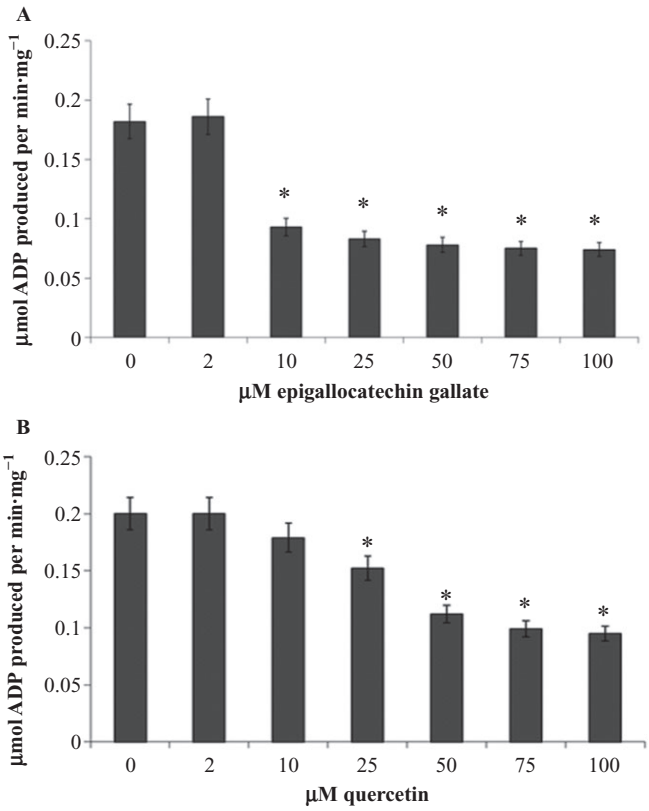

Figure 5

ATP hydrolysis in purified OS with EGCG and quercetin. Histogram shows ATP hydrolysis over 1 min at 37°C, at pH 7.3, by OS (40µg·mL^{-1}). (A) Over a range of concentrations, EGCG (A) or quercetin (B) inhibit ATP hydrolysis in OS preparations. Data shown are means ± SD $n = 4$. *$P < 0.01$, paired Student's *t*-test.

ROI produced by the ETC, may release this protein into the OS cytosol. This would cause apoptosis mediated by activation of the apoptosome, composed of caspase 9 and Apaf-1 (Blanch *et al.*, 2014)], triggering the caspase-dependent cell death pathway. Therefore, we confirmed the presence of apoptosomes in the OS and their possible activation. Figure 8 shows that procaspase 9 (Figure 8A), procaspase 3 (Figure 8B) and Apaf-1 (Figure 8C) were present both in OS and in the cytosolic fraction (S9) used as positive control. Data were confirmed by immunogold TEM experiments on bovine retinal sections labelled with the same antibody used for Western blots (Figure 9). Immunoreactive procaspase 3 and procaspase 9 were clearly present in OS, where they colocalized with immunoreactive signals for rhodopsin. The two anti-procaspase 3 and 9 antibodies also labelled the IS mitochondria. Similarly, immunoreactive Apaf-1 was observed in OS and IS mitochondria.

Discussion and conclusion

The present data show that, in the OS, resveratrol and curcumin inhibit the ATP synthase activity (Figure 4), while quercetin and EGCG inhibit the ATPase activity (Figure 5). This is in accordance with the report showing that polyphenols (which includes curcumin, resveratrol, quercetin and EGCG) act as inhibitors of the ATPase and/or ATP synthase activity of mitochondrial ATP synthase (Zheng and Ramirez, 2000). Notably, in our experimental system, these compounds were able to also inhibit oxygen consumption by the OS (Figure 6), indicating that they can affect the process of oxidative phosphorylation. Our data are consistent with the hypothesis that the OS express a functional ATP synthase as previously reported (Calzia *et al.*, 2013a). The significance of this finding is underlined by the observation that all polyphenols are not able to enter the intact mitochondrion, which needs to be treated with detergents or sonication in order to measure the effects of polyphenols on its ATPase or ATP synthase activities (Zheng and Ramirez, 2000).

A possible beneficial effect induced by polyphenols on several vision-threatening retinal diseases has already been reported (Gurib-Fakim, 2006; Panfoli *et al.*, 2012). Our hypothesis was that a protective effect of polyphenols on the retina would be mediated mainly by targeting the extramitochondrial ATP synthase in the OS. Being the F_1 moiety of ATP synthase faces the outside of the OS disk (Panfoli *et al.*, 2008; 2009), the polyphenol compounds would have direct access to their binding side on F_1 moiety of ATP synthase of the disk.

Antioxidant therapies reduced the incidence of the oxidative stress-related AMD (Khandhadia and Lotery, 2010) and *in vivo* studies with rat models of DR have shown direct benefits from oral administration of curcumin (Gupta *et al.*, 2011). Curcumin is considered an effective compound for the treatment and prevention of AMD and DR (Huynh *et al.*, 2013), however such efficacy was shown only at higher doses, with potential side effects. Our data showed that the antioxidative action of curcumin was potentiated by the co-administration of piperine (Figure 4), suggesting that the latter not only improves the bioavailability of curcumin by blocking its metabolic degradation (Anand *et al.*, 2007), but may also be involved in its pharmacological action. Intraocular injection of EGCG with sodium nitroprusside showed a protective effect on the retinal photoreceptors (Zhang and Osborne, 2006). Oral administration of EGCG reduced light-induced retinal neuronal death, suggesting some efficacy in preventing photoreceptor cell death (Costa *et al.*, 2008; Zhang *et al.*, 2008). *In vivo*, quercetin treatment decreased choroidal neovascularization size in a laser-induced model of AMD (Zhuang *et al.*, 2011).

The mode of action of resveratrol in blocking the F_1 moiety of ATP synthase is similar to that of the endogenous IF_1 (Gledhill *et al.*, 2007) and of aurovertin B, both inhibitors of mitochondrial ATP synthase (Huang *et al.*, 2008). As ATP synthase is a nanomotor, these compounds inhibit ATP synthase by inserting between the α and β subunits, in the F_1 moiety. Interestingly, cytofluorimetric data showed that resveratrol did not discharge the proton potential in the OS disk membranes (Table 1). This confirms the finding that resveratrol does not permanently inactivate ATP synthase, as it is a reversible inhibitor of F_1 moiety, because its binding occurs in the aqueous phase (Gledhill *et al.*, 2007). In this way, resveratrol would not act as a scavenger antioxidant, but rather as a modulator of electron flux inside the ETC. As the ETC is coupled to the synthesis of ATP for membrane integrity, the

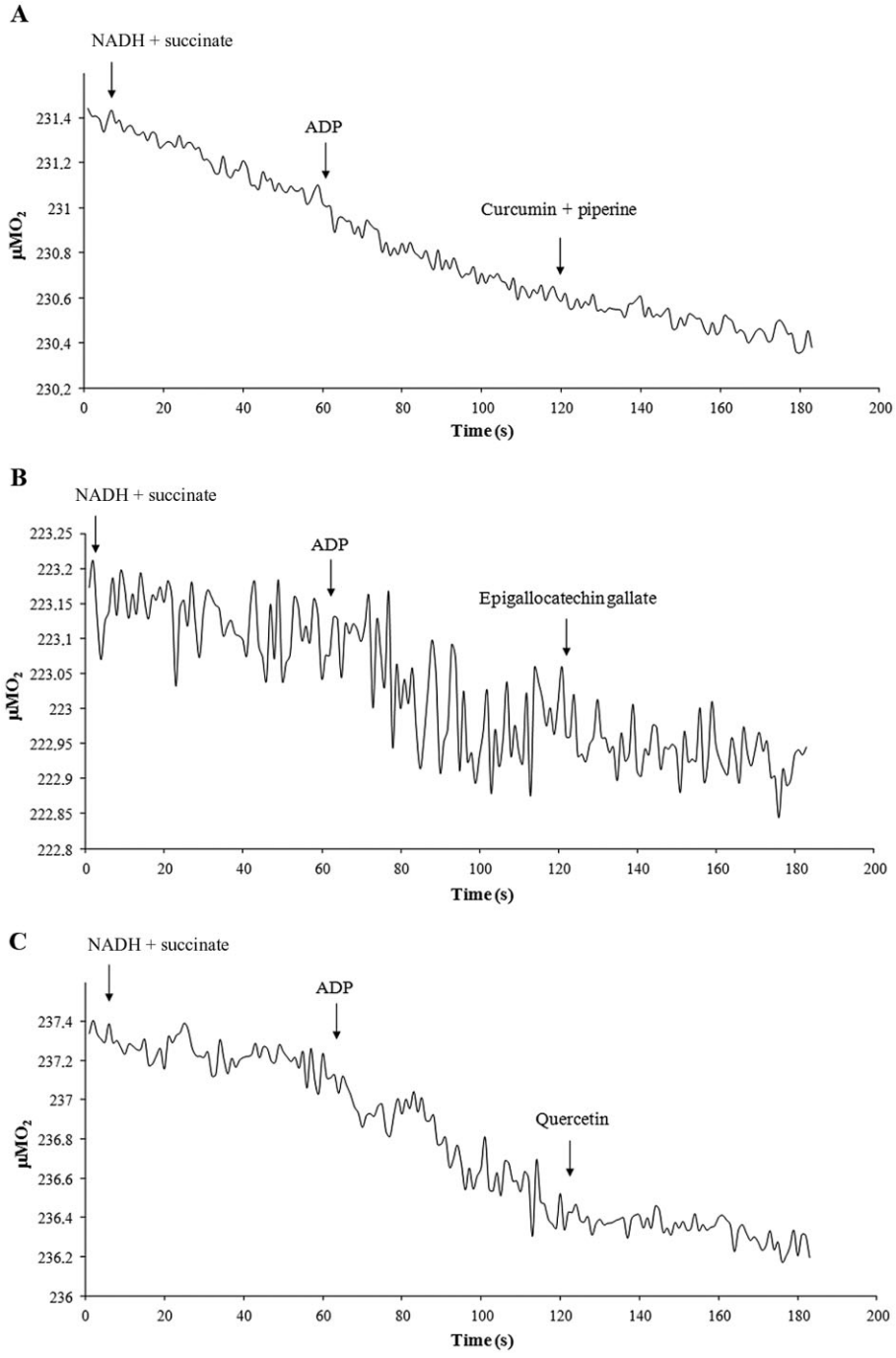

Figure 6

Measurements of respiration rates in purified rod OS in the presence of curcumin, EGCG or quercetin. Representative amperometric recording traces of coupled respiration rates in OS. Additions were NADH (0.2 mM), succinate (20 mM) and ADP (0.1 mM). Then in (A), curcumin and piperine (100 µM); in (B), EGCG (100 µM) and in (C) quercetin (100 µM), were added. About 40 µg of total OS proteins were used in 1.7 mL reaction volume.

production of ROI by the ETC is proportional to its function. Resveratrol would indirectly decrease the ETC activity and nutrient utilization, modulating ROI production by reversibly inhibiting ATP synthase without discharging the proton potential. This polyphenol which is found in grapes and wine, was reported to reduce vascular lesions and oxidative stress in DR in rat and mouse models (Lu *et al.*, 2006; Kim *et al.*, 2012). Protection against injury-induced capillary degeneration by resveratrol has also been demonstrated (Lu *et al.*, 2006). Treatment of whole cells with resveratrol for some days partly restored the Fanconi anaemia mitochondrial metabolic activity while decreasing oxygen uptake in

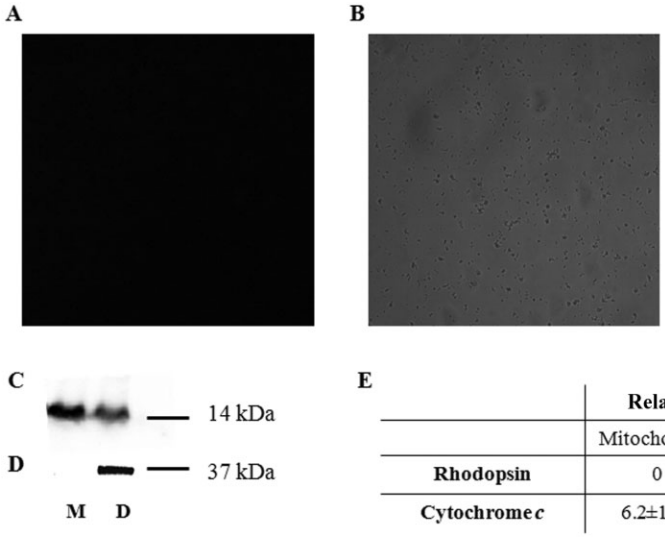

E

	Relative optical density	
	Mitochondria	Disks
Rhodopsin	0	8.7±1.05
Cytochrome *c*	6.2±1.24	4.13±0.6

Figure 7

Expression of Cyt *c* in disks. (A) CLSM image of Cy3 indirect fluorescence of Cyt *c*. (B) Transmission image of disks represented in (A). (C) Semi-quantitative Western blot analysis of rhodopsin (Rh) in disks (D) and mitochondria-enriched fraction (M). (D) Semi-quantitative Western blot analysis of Cyt *c* in disks (D) and mitochondria-enriched fraction (M). (E) Densitometric analysis made with ChemiDoc software (Bio-Rad Laboratories). Each value is the mean ± S.D; $n = 5$.

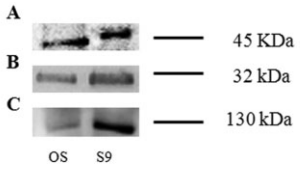

D

	Relative optical density	
	OS	S9
Procaspase 9	4.1±0.61	5.4±0.86
Procaspase 3	3.2±0.45	3.7±0.56
Apaf-1	2.4±0.41	4.8±0.73

Figure 8

Semi-quantitative Western blot analysis of procaspase 9, procaspase 3 and Apaf-1. Panels (A–C) are semi-quantitative Western blot signal of Ab anti-procaspase 9, procaspase 3 and Apaf-1. Samples are isolated OS and mitochondria-enriched fraction (M). Panel (D) is a densitometric analysis made with ChemiDoc software (Bio-Rad Laboratories). Each value is the mean ± S.D; $n = 6$.

wild-type cells (Columbaro *et al.*, 2014). The effects of N,N_-dicyclohexylcarbodiimide and oligomycin are different as they act on the F_o moiety in the lipid phase (Morelli *et al.*, 2013).

Our data show that H_2O_2 was produced in the purified rod OS as a direct consequence of its respiratory ability (Table 2) and that the level of MDA, a well-established biomarker of lipid peroxidation and oxidative stress, increased in the OS in the presence of NADH, a substrate of the respiratory complex I (Table 1). The presence of an active ETC in the OS (Panfoli *et al.*, 2009; Calzia *et al.*, 2013a; 2014) should then be considered a primary site of ROI generation. In fact, the respiratory complex I is a major source of ROI (Genova *et al.*, 2008). This supports the theory that disk membrane lipids are peroxidized because of the ROI production by the ectopic ETC. A faster functioning of the ETC in the outer limb is expected in case of sustained illumination, which would produce more ROI (Panfoli *et al.*, 2012). This is consistent with data reporting that when phototransduction is persistently activated, as during continuous intense blue-light illumination (Roehlecke *et al.*, 2013), oxidative stress increases in the rod OS.

In rat models of light-induced retinal degeneration, curcumin supplementation was neuroprotective (Mandal *et al.*, 2009) against ROI production (Woo *et al.*, 2012). Quercetin induced dose-dependent inhibition of cellular migration and tube formation, important steps in retinal angiogenesis characteristic of AMD, and reduced cellular oxidative damage and senescence (Kook *et al.*, 2008), inhibiting ROI production in retinal cell cultures (Areias *et al.*, 2001). A key role for ROI in retinal degeneration processes such as AMD, DR, cataract and glaucoma has been suggested, because photoreceptors are particularly sensitive to oxidative stress (Liang and Godley, 2003).

Further support for the involvement of ROI generation and oxidative stress in photoreceptor apoptosis comes from studies in which antioxidants appear to retard or inhibit the degenerative process (Lam *et al.*, 1990; Ranchon *et al.*, 1999). Apoptosis seems to be responsible for the cell loss seen in several disorders of the retina, including retinitis pigmentosa (RP), glaucoma and macular degeneration (Dunaief *et al.*, 2002; Carella, 2003) and some protective effects of quercetin were mediated by direct inhibition of the intrinsic apoptosis pathway (Cao *et al.*, 2010).

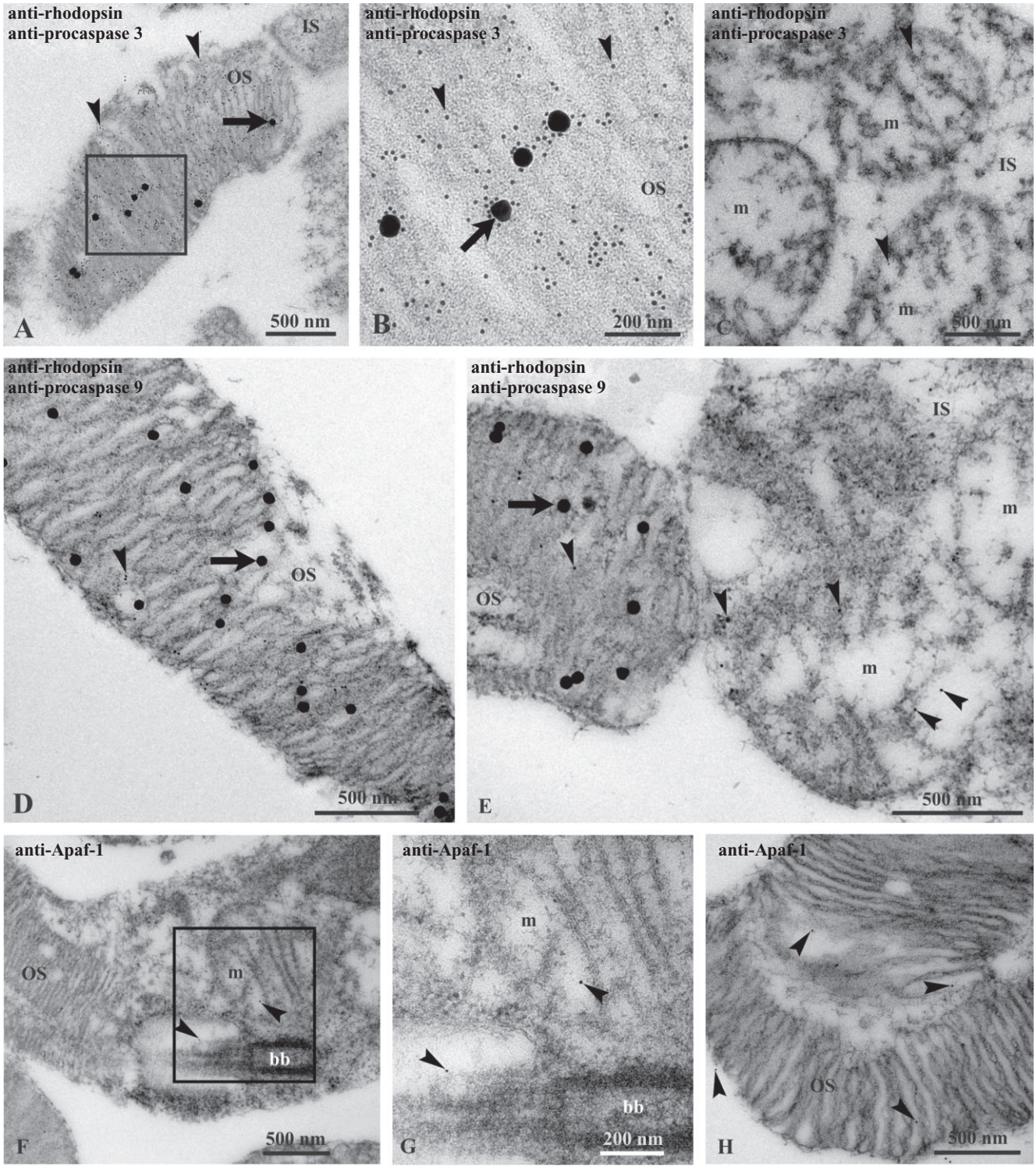

Figure 9

TEM of bovine retina. Procaspase 3 (A–C), procaspase 9 (D–E) and Apaf-1 (F–H) expression. (A–E) The retina is double-labelled with antibodies against rhodopsin (Rh; large, 40 nm width gold particles; arrows) and against procaspase 3 or against procaspase 9 (small, 10 nm width gold particles; arrowheads). (A–B) A preparation of OS. Squared area in (A) is enlarged in (B) to show a magnification of OS disks expressing both rhodopsin and procaspase 3. (C) Three mitochondria (m) in IS expressing procaspase 3. (D) An OS showing expression of both Rh and procaspase 9. (E) Rod junction area between the OS (left) and the IS (right). In OS disks, anti-Rh and anti-procaspase 9 colocalize; in mitochondria (m), only procaspase 9 is visualized. (F–G) Rod junction area between the OS (left) and the IS (right) exhibiting Apaf-1 expression (arrowheads) both in OS and in IS. Squared area in (F) is enlarged in (G) to show a magnification of a labelled mitochondria and in the cytosol close to the ciliary basal body (bb). (H) An OS showing expression of Apaf-1 (arrowheads).

Our results show that Cyt *c* was localized inside the disk membrane (Figure 8), consistent with our proteomic studies reporting its presence in purified disks (Panfoli *et al.*, 2008). The expression of procaspase 9, procaspase 3 (Figure 8) and Apaf-1 in the OS showed that these molecules involved in the first step of apoptosis are all present in this tissue. The initiator caspase-9 is activated in response to stimuli that lead to Cyt *c* release from mitochondria and is essential for the initiation of the caspase cascade, whereas caspase-3 is considered to be the main executioner of apoptosis (Slee *et al.*, 1999). Caspase-3 involvement in photoreceptor apoptosis has been reported (Kim *et al.*, 2002; Wu *et al.*, 2002). Thus the caspase-dependent, cell death machinery may be present in the OS and could be initiated by the extrusion of Cyt *c* from the disk when its membrane is damaged by oxidation. This oxidation would be generated by the ROI produced by the hyperactivity of the respiratory chains.

In conclusion, our data suggest a possible molecular mechanism of action of polyphenolic phytochemicals, by reducing ROI production through modulation of the extramitochondrial ATP synthase in the OS. Under pathological conditions, uncoupled functioning of oxidative phosphorylation or functional ETC overload could damage the disk membrane causing the release of Cyt *c*, triggering apoptosis in the rods, typical of rod dystrophies such as RP and AMD (Dunaief *et al.*, 2002). Further studies are needed to assess whether the modulation of ATP synthase in retinal rods is a primary mode of action of polyphenol compounds. This would offer a scientific validation for the use of such compounds as adjuvant treatment in the therapy of oxidative stress-related retinopathies.

Acknowledgments

We thank Ersilia M. D'Aste, veterinarian of Genova's slaughterhouse, for giving us authorization to obtain bovine retinas.

Author contributions

D. C. and M. O. performed the biochemical analysis (oxymetry and ATP synthesis and hydrolysis analysis) and analysed and interpreted the results. F. C. performed TEM immunogold experiments on bovine eye sections. P. B. performed confocal imaging acquisition. S. R. and M. B. performed Western blotting analysis. A. D. provided expertise of confocal imaging analysis. P. D. performed, analysed and interpreted cytofluorimetric analysis. L. M. provided expertise of TEM immunogold analysis on bovine eye sections and analyse and interpreted the results. C. E. T. provided clinical expertise, contributed to the analysis of the data, discussed prepublication results and reviewed the manuscript. D. C. performed graphic illustration, analysis of the data and wrote the paper. I. P. designed the research study, performed analysis of the data and wrote the paper.

Conflicts of interest

None to declare.

References

Aicardi G, Solaini G (1982). Effects of niridazole and 5-nitroimidazoles on heart mitochondrial respiration. Biochem Pharmacol 31: 3703–3705.

Alexander SPH, Benson HE, Faccenda E, Pawson AJ, Sharman JL Spedding M *et al.* (2013). The Concise Guide to PHARMACOLOGY 2013/14: Enzymes. Br J Pharmacol 170: 1797–1867.

Anand P, Kunnumakkara AB, Newman RA, Aggarwal BB (2007). Bioavailability of curcumin: problems and promises. Mol Pharm 4: 807–818.

Areias FM, Rego AC, Oliveira CR, Seabra RM (2001). Antioxidant effect of flavonoids after ascorbate/Fe(2+)-induced oxidative stress in cultured retinal cells. Biochem Pharmacol 62: 111–118.

Baynes JW (1991). Role of oxidative stress in development of complications in diabetes. Diabetes 40: 405–412.

Berman SB, Watkins SC, Hastings TG (2000). Quantitative biochemical and ultrastructural comparison of mitochondrial permeability transition in isolated brain and liver mitochondria: evidence for reduced sensitivity of brain mitochondria. Exp Neurol 164: 415–425.

Bianchini P, Calzia D, Ravera S, Candiano G, Bachi A, Morelli A *et al.* (2008). Live imaging of mammalian retina: rod outer segments are stained by conventional mitochondrial dyes. J Biomed Opt 13: 54017.

Blanch RJ, Ahmed Z, Thompson AR, Akpan N, Snead DRJ, Berry M *et al.* (2014). Caspase-9 mediates photoreceptor death after blunt ocular trauma. Invest Ophthalmol Vis Sci 55: 6350–6357.

Boyer PD (1997). The ATP synthase – a splendid molecular machine. Annu Rev Biochem 66: 717–749.

Bucher T, Pfleiderer G (1955). Pyruvate kinase from muscle. Methods Enzymol 1: 435–440.

Calzia D, Barabino S, Bianchini P, Garbarino G, Oneto M, Caicci F *et al.* (2013a). New findings in ATP supply in rod outer segments: insights for retinopathies. Biol Cell 105: 345–358.

Calzia D, Candiani S, Garbarino G, Caicci F, Ravera S, Bruschi M *et al.* (2013b). Are rod outer segment ATP-ase and ATP-synthase activity expression of the same protein? Cell Mol Neurobiol 33: 637–649.

Calzia D, Garbarino G, Caicci F, Manni L, Candiani S, Ravera S *et al.* (2014). Functional expression of electron transport chain complexes in mouse rod outer segments. Biochimie 102: 78–82.

Cao X, Liu M, Tuo J, Shen D, Chan CC (2010). The effects of quercetin in cultured human RPE cells under oxidative stress and in Ccl2/Cx3cr1 double deficient mice. Exp Eye Res 91: 15–25.

Carella G (2003). Introduction to apoptosis in ophthalmology. Eur J Ophthalmol 13 (Suppl. 3): S5–S10.

Chinopoulos C, Starkov AA, Fiskum G (2003). Cyclosporin A-insensitive permeability transition in brain mitochondria: inhibition by 2-aminoethoxydiphenyl borate. J Biol Chem 278: 27382–27389.

Columbaro M, Ravera S, Capanni C, Panfoli I, Cuccarolo P, Stroppiana G *et al*. (2014). Treatment of FANCA cells with resveratrol and N-acetylcysteine: a comparative study. PLoS ONE 9: e104857.

Costa BL, Fawcett R, Li GY, Safa R, Osborne NN (2008). Orally administered epigallocatechin gallate attenuates light-induced photoreceptor damage. Brain Res Bull 76: 412–423.

Dunaief JL, Dentchev T, Ying GS, Milam AH (2002). The role of apoptosis in age-related macular degeneration. Arch Ophthalmol 120: 1435–1442.

Fain GL, Matthews HR, Cornwall MC, Koutalos Y (2001). Adaptation in vertebrate photoreceptors. Physiol Rev 81: 117–151.

Fliesler SJ, Anderson RE (1983). Chemistry and metabolism of lipids in the vertebrate retina. Prog Lipid Res 22: 79–131.

Genova ML, Baracca A, Biondi A, Casalena G, Faccioli M, Falasca AI *et al*. (2008). Is supercomplex organization of the respiratory chain required for optimal electron transfer activity? Biochim Biophys Acta 1777: 740–746.

Gledhill JR, Montgomery MG, Leslie AG, Walker JE (2007). Mechanism of inhibition of bovine F1-ATPase by resveratrol and related polyphenols. Proc Natl Acad Sci U S A 104: 13632–13637.

Gupta SK, Kumar B, Nag TC, Agrawal SS, Agrawal R, Agrawal P *et al*. (2011). Curcumin prevents experimental diabetic retinopathy in rats through its hypoglycemic, antioxidant, and anti-inflammatory mechanisms. J Ocul Pharmacol Ther 27: 123–130.

Gurib-Fakim A (2006). Medicinal plants: traditions of yesterday and drugs of tomorrow. Mol Aspects Med 27: 1–93.

Higdon JV, Frei B (2003). Tea catechins and polyphenols: health effects, metabolism, and antioxidant functions. Crit Rev Food Sci Nutr 43: 89–143.

Huang TC, Chang HY, Hsu CH, Kuo WH, Chang KJ, Juan HF (2008). Targeting therapy for breast carcinoma by ATP synthase inhibitor aurovertin B. J Proteome Res 7: 1433–1444.

Huynh T-P, Mann SN, Mandal NA (2013). Botanical compounds: effects on major eye diseases. Evid Based Complement Alternat Med 2013: 549174.

Janik-Papis K, Ulińska M, Krzyzanowska A, Stoczynska E, Borucka AI, Wozniak K *et al*. (2009). Role of oxidative mechanisms in the pathogenesis of age-related macular degeneration. Klin Oczna 111: 168–173.

Khandhadia S, Lotery A (2010). Oxidation and age-related macular degeneration: insights from molecular biology. Expert Rev Mol Med 12: e34.

Kim DH, Kim JA, Choi JS, Joo CK (2002). Activation of caspase-3 during degeneration of the outer nuclear layer in the rd mouse retina. Ophthalmic Res 34: 150–157.

Kim YH, Kim YS, Roh GS, Choi WS, Cho GJ (2012). Resveratrol blocks diabetes-induced early vascular lesions and vascular endothelial growth factor induction in mouse retinas. Acta Ophthalmol 90: e31–e37.

Kook D, Wolf AH, Yu AL, Neubauer AS, Priglinger SG, Kampik A *et al*. (2008). The protective effect of quercetin against oxidative stress in the human RPE *in vitro*. Invest Ophthalmol Vis Sci 49: 1712–1720.

Laemmli UK (1970). Cleavage of structural proteins during the assembly of the head of bacteriophage T4. Nature 227: 680–685.

Lam S, Tso MO, Gurne DH (1990). Amelioration of retinal photic injury in albino rats by dimethylthiourea. Arch Ophthalmol 108: 1751–1757.

Lang DR, Racker E (1974). Effects of quercetin and F1 inhibitor on mitochondrial ATPase and energy-linked reactions in submitochondrial particles. Biochim Biophys Acta 333: 180–186.

Lee SR, Im KJ, Suh SI, Jung JG (2003). Protective effect of green tea polyphenol (-)-epigallocatechin gallate and other antioxidants on lipid peroxidation in gerbil brain homogenates. Phytother Res 17: 206–209.

Liang FQ, Godley BF (2003). Oxidative stress-induced mitochondrial DNA damage in human retinal pigment epithelial cells: a possible mechanism for RPE aging and age-related macular degeneration. Exp Eye Res 76: 397–403.

Linnett PE, Beechey RB (1979). Inhibitors of the ATP synthethase system. Methods Enzymol 55: 472–518.

Linsenmeier RA, Braun RD, McRipley MA, Padnick LB, Ahmed J, Hatchell DL *et al*. (1998). Retinal hypoxia in long-term diabetic cats. Invest Ophthalmol Vis Sci 39: 1647–1657.

Lu KT, Chiou RY, Chen LG, Chen MH, Tseng WT, Hsieh HT *et al*. (2006). Neuroprotective effects of resveratrol on cerebral ischemia-induced neuron loss mediated by free radical scavenging and cerebral blood flow elevation. J Agric Food Chem 54: 3126–3131.

Mandal MN, Patlolla JM, Zheng L, Agbaga MP, Tran JT, Wicker L *et al*. (2009). Curcumin protects retinal cells from light-and oxidant stress-induced cell death. Free Radic Biol Med 46: 672–679.

Mangiullo R, Gnoni A, Leone A, Gnoni GV, Papa S, Zanotti F (2008). Structural and functional characterization of F(o)F(1)-ATP synthase on the extracellular surface of rat hepatocytes. Biochim Biophys Acta 1777: 1326–1335.

Morelli AM, Ravera S, Calzia D, Panfoli I (2013). Hypothesis of lipid-phase-continuity proton transfer for aerobic ATP synthesis. J Cereb Blood Flow Metab 33: 1838–1842.

Panfoli I, Musante L, Bachi A, Ravera S, Calzia D, Cattaneo A *et al*. (2008). Proteomic analysis of the retinal rod outer segment disks. J Proteome Res 7: 2654–2669.

Panfoli I, Calzia D, Bianchini P, Ravera S, Diaspro A, Candiano G *et al*. (2009). Evidence for aerobic metabolism in retinal rod outer segment disks. Int J Biochem Cell Biol 41: 2555–2565.

Panfoli I, Calzia D, Ravera S, Morelli AM, Traverso CE (2012). Extra-mitochondrial aerobic metabolism in retinal rod outer segments: new perspectives in retinopathies. Med Hypotheses 78: 423–427.

Pawson AJ, Sharman JL, Benson HE, Faccenda E, Alexander SP, Buneman OP *et al*.; NC-IUPHAR (2014). The IUPHAR/BPS Guide to PHARMACOLOGY: an expert-driven knowledge base of drug targets and their ligands. Nucl Acids Res 42 (Database Issue): D1098–D1106.

Pedersen PL, Amzel LM (1993). ATP synthases. Structure, reaction center, mechanism, and regulation of one of nature's most unique machines. J Biol Chem 268: 9937–9940.

van Raaij MJ, Abrahams JP, Leslie AG, Walker JE (1996). The structure of bovine F1-ATPase complexed with the antibiotic inhibitor aurovertin B. Proc Natl Acad Sci U S A 93: 6913–6917.

Ranchon I, Gorrand JM, Cluzel J, Droy-Lefaix MT, Doly M (1999). Functional protection of photoreceptors from light-induced damage by dimethylthiourea and *Ginkgo biloba* extract. Invest Ophthalmol Vis Sci 40: 1191–1199.

Ravera S, Calzia D, Bianchini P, Diaspro A, Panfoli I (2007). Confocal laser scanning microscopy of retinal rod outer segment intact disks: new labeling technique. J Biomed Opt 12: 050501.

Roehlecke C, Schumann U, Ader M, Brunssen C, Bramke S, Morawietz H *et al*. (2013). Stress reaction in outer segments of photoreceptors after blue light irradiation. PLoS ONE 8: e71570.

Schnetkamp PP (1981). Metabolism in the cytosol of intact isolated cattle rod outer segments as indicator for cytosolic calcium and magnesium ions. Biochemistry 20: 2449–2456.

Schnetkamp PP, Daemen FJ (1982). Isolation and characterization of osmotically sealed bovine rod outer segments. Methods Enzymol 81: 110–116.

Slee EA, Harte MT, Kluck RM, Wolf BB, Casiano CA, Newmeyer DD *et al*. (1999). Ordering the cytochrome c-initiated caspase cascade: hierarchical activation of caspases-2, -3, -6, -7, -8, and -10 in a caspase-9-dependent manner. J Cell Biol 144: 281–292.

Stefansson E (2006). Ocular oxygenation and the treatment of diabetic retinopathy. Surv Ophthalmol 51: 364–380.

Stock D, Leslie AG, Walker JE (1999). Molecular architecture of the rotary motor in ATP synthase. Science 286: 1700–1705.

Wangsa-Wirawan ND, Linsenmeier RA (2003). Retinal oxygen: fundamental and clinical aspects. Arch Ophthalmol 121: 547–557.

Woo JM, Shin DY, Lee SJ, Joe Y, Zheng M, Yim JH *et al*. (2012). Curcumin protects retinal pigment epithelial cells against oxidative stress via induction of heme oxygenase-1 expression and reduction of reactive oxygen. Mol Vis 18: 901–908.

Wu J, Gorman A, Zhou X, Sandra C, Chen E (2002). Involvement of caspase-3 in photoreceptor cell apoptosis induced by *in vivo* blue light exposure. Invest Ophthalmol Vis Sci 43: 3349–3354.

Zanotti F, Gnoni A, Mangiullo R, Papa S (2009). Effect of the ATPase inhibitor protein IF1 on H+ translocation in the mitochondrial ATP synthase complex. Biochem Biophys Res Commun 384: 43–48.

Zhang B, Osborne NN (2006). Oxidative-induced retinal degeneration is attenuated by epigallocatechin gallate. Brain Res 1124: 176–187.

Zhang B, Rusciano D, Osborne NN (2008). Orally administered epigallocatechin gallate attenuates retinal neuronal death *in vivo* and light-induced apoptosis *in vitro*. Brain Res 1198: 141–152.

Zheng J, Ramirez VD (2000). Inhibition of mitochondrial proton F0F1-ATPase/ATP synthase by polyphenolic phytochemicals. Br J Pharmacol 130: 1115–1123.

Zhuang P, Shen Y, Lin BQ, Zhang WY, Chiou GC (2011). Effect of quercetin on formation of choroidal neovascularization (CNV) in age-related macular degeneration (AMD). Eye Sci 26: 23–29.